

IoT Utilized Gas-Leakage Monitoring System with Adaptive Controls Applicable to Dual Fuel Powered Naval Vessels/Ships: Development & Implementation

Avijit Mallik¹, Sharif Ahmed^{2,3}, G. M. M. Hossain⁴, M. R. Rahman¹

¹Department of Mechanical Engineering, RUET, Rajshahi 6204, Bangladesh

²Department of Marine Engineering, Marine Fisheries Academy, Chattogram 4000, Bangladesh

³Department of Naval Architecture and Ocean Engineering, WUT, Wuhan, Hubei Province, China

⁴Department of Electrical & Electronic Engineering, RUET, Rajshahi 6204, Bangladesh

E-mails: avijitme13@gmail.com sharifahmedmfa@whut.edu.cn gmmehedi.eee10@gmail.com

Abstract: Leakage of Liquefied Petroleum Gas and Liquefied Natural Gas (LPG/LNG) produces hazardous and toxic impact on humans and other living creatures. The authors developed a system to monitor and control the gas leakage concentration. MQ-6 gas sensor is used for sensing the level of gas concentration in a closed volume. To monitor the consequences of environmental changes an IoT platform hosted by “Thingspeak” platform has been introduced. Both robust and cloud-forwarded controls have been applied to prevent uncontrolled leakage of those gases and auto-ignition. This type of system can be directly applied to the engine chamber/fuel chamber of the modern marine vessels using dual fuel power cycle with LPG/LNG as secondary fuel-flamer. The results from the experiments clearly indicate satisfactory actuation speed and accuracy. The trials performed by the authors showed about 99% efficiency of signal transmission and actuation.

Keywords: Internet of Things, Smart System, Gas Leakage Control, Embedded System.

1. Introduction

Semiconductor based metal dioxide gas sensors are very well known for their availability, ease of use along with high sensitivity. Those sensors are mostly used in industries and automobiles (vehicles and ships). Those sensors can give very precise response under closed control volume conditions (closed system), but its signal fluctuates when the temperature and relative humidity of the control volume crosses the specified limits (25-30 °C temperature and 55-65% RH). But those sensors also fluctuate in a constant proportional limit which can be subjected to model calibration and about 95% precise calibrations can be made using some proved signal processing simulations. Thus, from the bad sensor signals, the actual signals can be predicted.

However, those sensors are used extensively in various applications like Electronic nose (E-nose) to detect specific range of gases [5, 6], odor localization [7-9], plume tracking [10, 11], etc. These sensors have a different response level [12] with respect to variation of temperature, relative humidity, and gas odor concentration. The mathematical models based on these responses have been the aim of researchers for understanding sensor's behavior and the system in which sensors are included.

Emission regulation is a very key technical issues for marine engines for its direct contact with marine environment and LNG/LPG is becoming increasingly attractive for its availability and low price compared to other gaseous engines. Normally used marine engines have high Sulphur (over 1-5%) contents in its exhaust gases which is very harmful to human and marine environment. To reduce the Sulphur emission modern marine engines uses both diesel and LPG/LNG (as a secondary fuel) combinedly (known as dual fuel marine engines) or distilled Marine Diesel Oil (MDO). The second option is far more costly than dual fuel cycle powered fuels and are less Sulphur emissive. LPG and LNG are the key sources of substitutable powers in recent days for its availability and ease of transportation. Those are utilized as a substitute fuel in dual fuel cycle powered engines (used in vehicles and modern ships). The main challenge of sensing those LPG and LNG gas leakage is its unrecognizable odor (cannot be sensed by human nose in times of low concentration) and colorless form in normal conditions. Thus, embedded system is the only choice to design the leakage monitoring system for those types of gases. Accidents due to gas leakage are increasing in recent times. Inherently, the researchers focused their attention on developing a smart embedded system to monitor and avoid the gas leakage incidents in off-boarded ships which are subjected to repairing/maintenance [4]. Gas leakage detection is not only important but stopping leakage within smallest time interval is equally essential. The authors have designed and fabricated a system capable of sniffing LPG/LNG leakage based on volumetric concentration parts per million (ppm) and capable to undertake immediate actions to control the situation by utilizing Internet of Things (IoT).

For a long time, wireless technologies have been a real target of hackers due to the easiness of intercepting traffic and attacking without being noticed as some weaknesses in its security protocols [5]. Wireless Sensor Networking's (WSN) are also a big target due to the importance of the information it holds. For many wireless applications, the authentication system is relied on a Pre-Shared Key (PSK) which must be established before starting data communication between two or more devices. As a prevention, this research includes IoT utilized WSN's having developed State of Art (SoA) algorithms capable of detecting possible node capturing attacks along with timing delay measure technique to predict specific node viable to security threats [7, 8]. Industries and automobiles (vehicles and ships) utilizing gas-piping (Process, Pharmaceuticals, Chemical, Fuel-fired Power Plants and Dual Fuel Powered Marine Engine rooms, etc.) are considered as a reference to apply the proposed gas leakage monitoring and control utilizing WSN (IoT enabled with wireless HART) as per the experimental findings of the research undertaken. Table 1 shows some selected referred works on gas leakage/concentration detection and control in recent times (Table 1).

Table 1. Referred works on electronic sensor-based gas concentration detection and actuator control

Year	Purpose of research	Major findings	References
2014	Development of an Electronic nose for selected oil odor detection	In the new proposed method, the under damped natural frequency ω_n is calculated via considering the t_{rise} from 10% to 90% of the overshoot	[9]
2017	Development and analysis of GSM based gas leakage alerting system	Successful wireless GSM aided alerting for possible fire accidents	[10]
2017	Development of a wireless Electronic nose using artificial neural network for various gas concentration monitoring	Artificial neural network had been used to estimate the concentration of a gas in the air based on the ratio	[11]
2017	Internet of Things-based cargo monitoring system (IoT-CMS) to monitor any environmental changes	Introduced WSN and Fuzzy Logic Control simultaneously for the first time	[12]
2018	IoT based cold storage temperature and humidity monitoring	Showed how to control actuators over the net by just changing the state wise parameters from 0 to 1 and vice versa for controlling	[13]
2019	Gas leakage monitoring and swift adaptive control options for industrial automation	The data and control were hosted in an online IoT platform. The IoT platform provides real-time monitoring and control via “Thingspeak”	[14]

The literatures stated above were mainly focused on sensing environmental changes (like gas concentration, relative humidity of soil and air), but all of those recent works lags in swift feedforward control along with the Digital Signal Processing (DSP) and co-relation analysis (i.e., data coherence, stability of wireless data logging, noise filtering and, etc.). This paper involves, like previous literature sources where the authors have designed an automated LPG/LNG gas concentration monitoring system with both automatic and manual actuation from an IoT operated embedded platform. This research focuses on monitoring volumetric concentration (in parts per millions, ppm) of economic gaseous fuels like petroleum gases, liquid petroleum gas, carbon based toxic gases (high on carbon mono-oxide), etc., and to alert specific administrators/operators about the leakage through an IoT server (“Thingspeak”) provided with both automatic along with decision based actuator controlling to mitigate probable accidents from gas leakage. It also includes temperature and relative humidity sensing inside the control volume to check unstable sensory behavior as per the sensor datasheet.

2. Problem formulation

This research deals with monitoring LPG/LNG leakage along with administrative alert by switching specified relay(s) and sending an alert to administrator(s) to decide about the precautonal measures on basis of automation and feedforward command simultaneously. For this purpose, gas leakage concentration is sensed by gas sensor (MQ-6) which sends the data (analog) to the controller (NodeMCU) where the analog value is subjected to a sequential conversion to predict the probable intensity of gas inside the control volume and on crossing a reference threshold value (set by administrator/operator) the controller switches the relay(s) and alerting to the administrator/operator of the plant (Industry/Home) including an extra control-option

through manual control utilizing the IoT server to prevent accidents from the leakage. Figs 1 and 2 show the schematic block diagram and the experimental setup of the system, respectively. From the flow diagram (Fig. 1), it is noticed that the controller sets its Baud Rate or Sampling Frequency, Check Input-Output Pins, and the delay time/samples before starting sensory data-logging. Then the analog signal from gas sensor along with the digital signal from the relative humidity sensor is read and stored inside the read-only-memory of the controller for a specified timestamp constantly. The gas sensor data is subjected to Analog to Digital Conversion followed by voltage measurement from which the sensed gas concentration level is calibrated by means of coding. Then a comparator controls the feedback action and the wireless chip (ESP-8266) sends collected data to an authenticated server with an Internet Service activated router.

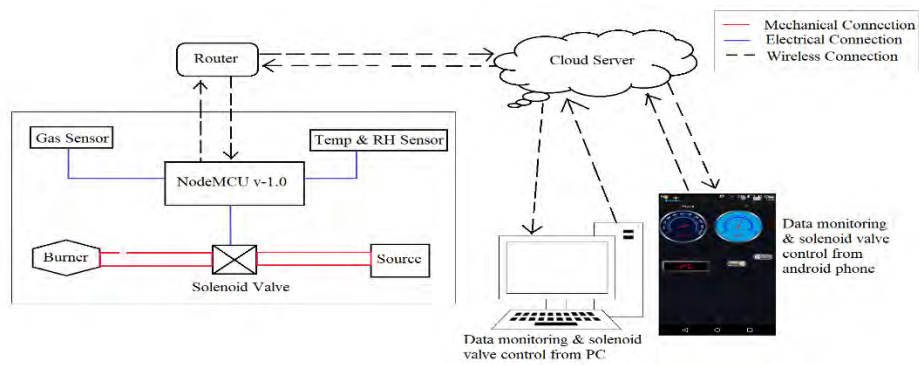


Fig. 1. System setup (schematic)

The system schematic shown in Fig. 1, is a graphical representation of the experimental system (Fig. 2). Here the NodeMCU used as controller is electrically connected to an analog sensor, a digital sensor and a high volt-amp rated actuator. The data transfer protocol used in this experiment is MQTT (Message Queuing Telemetry Transport); which is a low-space data transferring protocol widely used in wireless transmission.

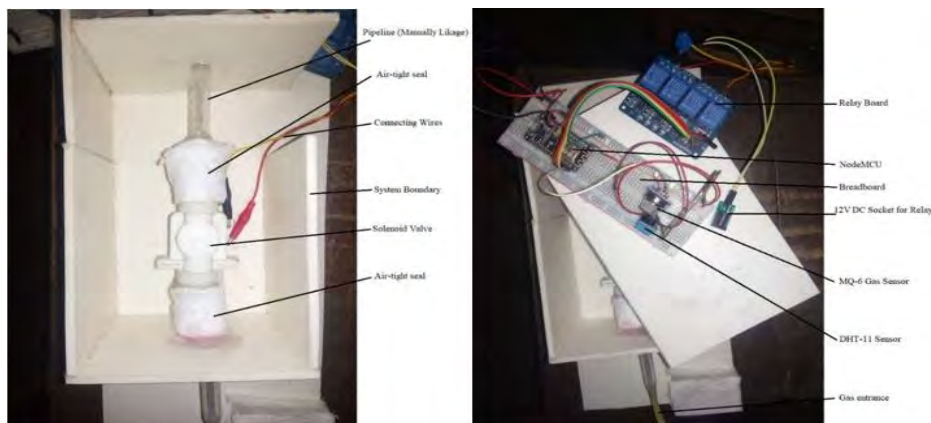


Fig. 2. Experimental setup

Fig. 3 depicts the total system networking. Firstly, the signals are obtained from analog/digital sensors and processed in the controller. Then the controller sends a continuous text command (String value) to the server where the main analytics takes place. All the conditions are programmed in the controller and the host server, so if any irregularities on collected data are observed then actions swiftly take place automatically or by manual decision.

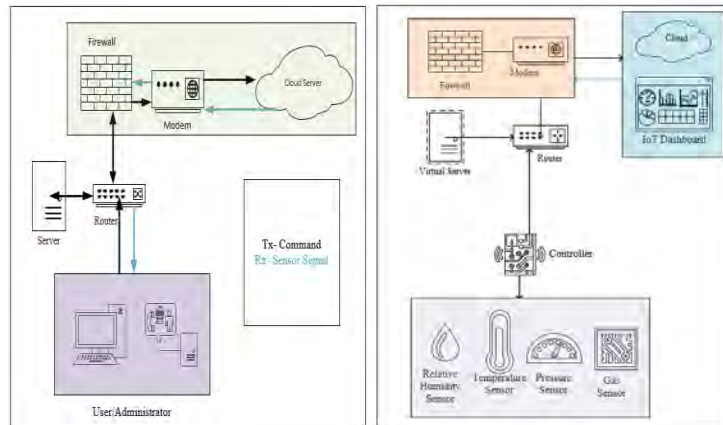


Fig. 3. System Networking (Schematic)

3. Mathematical model of sensory calibration

As the system focuses on gas concentration-based alerting and control of appliances, thus only MQ-6 gas sensor calibration (analog value to ppm) is considered for the mathematical analysis. DHT-11 sensor is to for checking the conditional Temperature and Relative Humidity as per gas sensor's datasheet. The gas sensor circuit schematic is shown in Fig. 4.

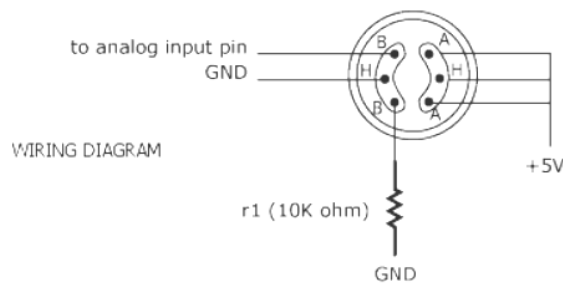


Fig. 4. MQ-6 gas sensor equivalent circuit schematic

Let, $V_C = \text{Supply Voltage} = +5 \text{ V}$, $R_S = \text{Sensor Resistance}$, $R_L = \text{Load Resistance (Variable)}$, $V_{RL} = \text{Sensor output Voltage}$. From current flow and voltage relationship

$$(1) \quad V = I \times R,$$

where $V = V_C$ & $R = R_S + R_L$, so, Equation (1) becomes to

$$(2) \quad I = \frac{V_C}{R_S + R_L}.$$

Again, from Equation (1):

$$(3) \quad V = I \times R; \text{ or, } V_{RL} = [V_c / (R_s + R_L)] \times R_L = \frac{(V_c \times R_L)}{(R_s + R_L)},$$

and from Equation (3),

$$(4) \quad V_{RL} \times (R_s + R_L) = V_c \times R_L; \text{ or, } R_s = [(V_c \times R_L) / V_{RL}] - R_L.$$

Upon simplification based on datasheet, the gas concentration can be determined directly in ppm (Parts per millions): Gas concentration, $C = [\text{Log}_{10}(\frac{R_s}{R_0}) - b] / m$ in parts per million (ppm) unit, where R_s/R_0 = Gas sensor sensitiveness, b = Interception from Y-axis (From, Sensor Datasheet; Sensitiveness vs PPM Graph), Slope(m) = $-(dy/dx)$. From, the equations of analog signals of 1024 (2^{10}) resolutions; Gas Sensor's Sensitivity = R_{s0}/R_0 , where, R_{s0} = Sensor Output Resistance at experimental environment, R_0 = Sensor Output Resistance at ideal environment (1000 ppm of LPG, 25 °C & 60% RH). At 32 °C & 55-65% of RH environment; Sensor Sensitivity, $R_{s0}/R_0 = 9.8$ (in fresh air for MQ-6) [14]. In this study, at 27 °C & 67% of RH environment; Sensor Sensitivity, $R_s/R_0 = 8.71$ (at normal room condition) is obtained from ADC [14, 15].

4. Experimental results and signal analysis

From experimental data, various calculations were performed using MATLAB environment. The Digital Signal Analysis-Toolbar is a great tool for signal processing and smoothing. As the data transfer took place using wireless media thus some additional noise was logged in an arbitrary manner. To overcome the problem a processing is needed. For this research, mainly Fast Fourier Transformation (FFT) was performed for better signal processing. The analysis procedure along with relative graphs are described below:

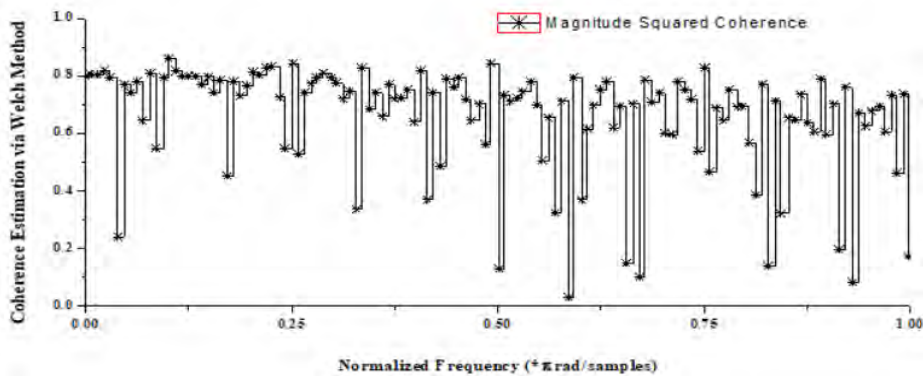


Fig. 5. Coherence estimation via Welch method

(i) **Coherence estimation via Welch method.** In digital signal processing, coherence is a statistic between two functions or signals which is used to estimate the power transfer of the input and output in a linear/linear time-invariant system. This algorithm is based on standard MATLAB's tools. The standard derivation of the mean is computed as [15-18],

$$(5) \quad \sigma(f) = \sqrt{2(1 - |Y(f)|^2)^2 / N |Y(f)|^2},$$

$$(6) \quad |Y(f)|^2 = |P_{xy}(f)|^2 / (P_{xx}(f) \cdot P_{yy}(f)).$$

If, $x(t)$ and $y(t)$ are two real value time variant functions where the coherence between the two signals is termed as $Y(f)$ (sometimes also called magnitude squared coherence) and $\sigma(f)$ is the standard deviation of the mean. By using Equations (5)-(6), Fig. 5 is plotted where a normalized frequency is used for better visualization which depicts the coherence estimation via Welch method. The figure shows that no data has been overlapped into one another, which verifies the continuous datalogging as quite satisfactory.

Fig. 6 denotes the magnitude response curve. The rms Signal-to-Noise Ratio (SNR) for an ideal N -bit converter is

$$(7) \quad \text{SNR} = 20 \log_{10} * \left(\text{r. m. s value of } F_s \frac{\text{input}}{r} \cdot \text{m. s value of quantization noise} \right),$$

or

$$(8) \quad \text{SNR} = 20 \log_{10} \frac{q^{2N} / 2 \sqrt{2}}{q / \sqrt{2}} = 20 \log_{10} 2^N + 20 \log_{10} \sqrt{\frac{3}{2}},$$

SNR = 6.02N + 1.76 dB, over the Nyquist bandwidth of interest.

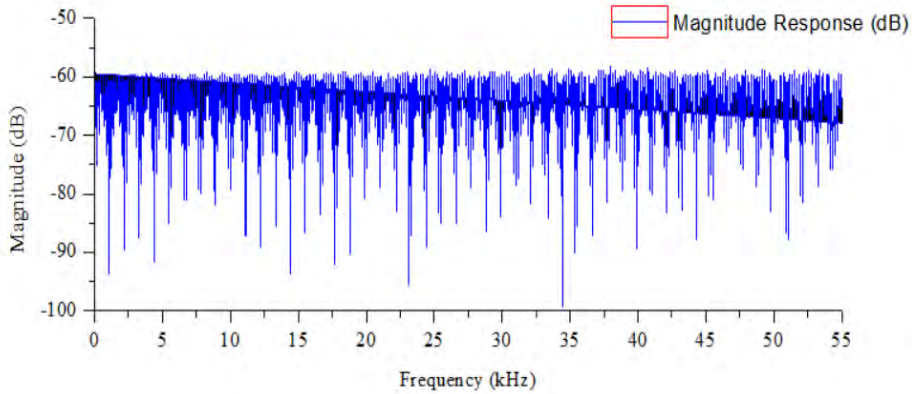


Fig. 6. Magnitude Response Graph (Gas sensor)

(ii) **Time-domain signal processing.** Now, using the gas sensor data Time-Domain graph was plotted in Fig. 7a to 8b, along with a 3rd and 8th order Fast Fourier Transformation (FFT) of the signal for better analysis. This is achieved, in a process known as convolution, by fitting successive sub-sets of adjacent data points with a low-degree polynomial by the method of linear least squares [19]. Fig. 7a depicts the plots of Raw analog, Savitzky-Golay Filtered value, moving average filtered value and the median plot.

Fig. 7b shows the Furrier fitted curve for gas sensor value from which the best suited filter was found to be the 5th order FFT. The higher and lower range has also been shown along with residuals plotted in black color. This signal filtration was done under room environment with no manual gas leak. By comparing the plots of Fig. 7, the 5th order FFT was finally considered as the filter for signal processing having very low range of residuals.

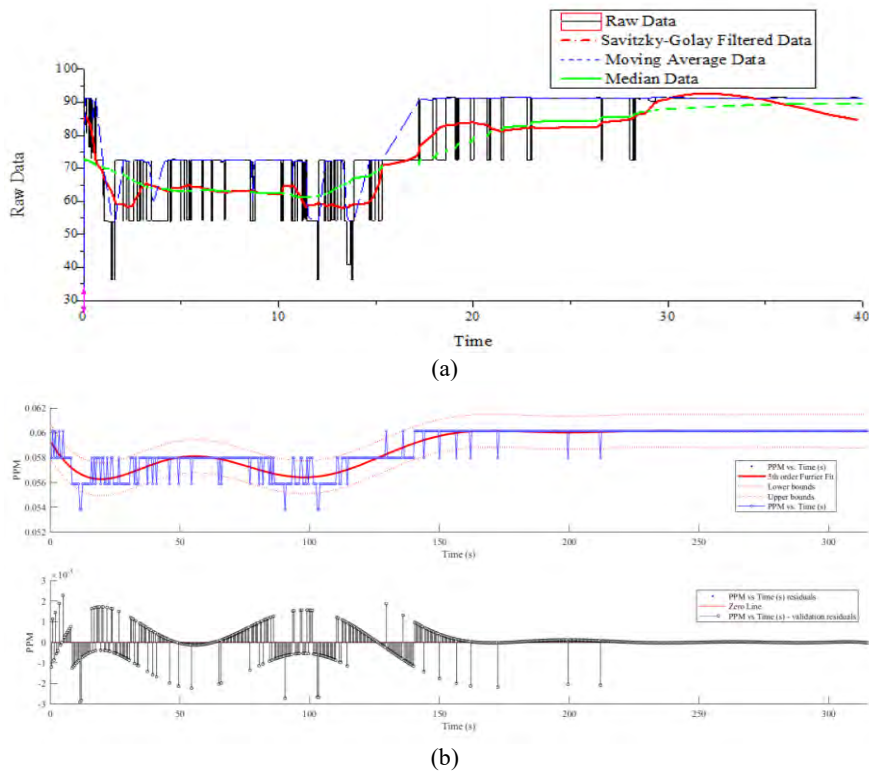


Fig. 7. Processed signal (PPM vs Time) (a); PPM vs Time Domain (5th order Furrier transforms with 95% confidence limit) (b)

The below Fig. 8a and b are the same plots as Fig. 7a and b, but those values represent the Temperature and Humidity. The same method of simulation was also considered for sensor's data smoothing with respect to time.

(iii) **Co-relation of multiple sensors signal.** The above two sections discuss various parameters based on single sensor prototype. But aligning multiple sensors' signals is very important to synchronize a total observation under a closed control volume. This research has also improvised on this keynote issue and found a sustainable solution to mitigate this major hindrance. Auto-correlation function for discrete time signals,

$$(9) \quad R(\tau) = \int x(t).x(t - \tau)dt.$$

From convolution theory, in time domain

$$(10) \quad R(\tau) = x(\tau) * x(-\tau)$$

for real functions $R(\tau)=R(-\tau)$, which proves the symmetry of autocorrelation. But this correlation function is in time domain and for analytical purpose it has to be changed into frequency domain or spectral domain. For this reason it must be Fourier transformed first, and then by inverse Fourier the same function can be again obtained, but this time it will be in frequency domain:

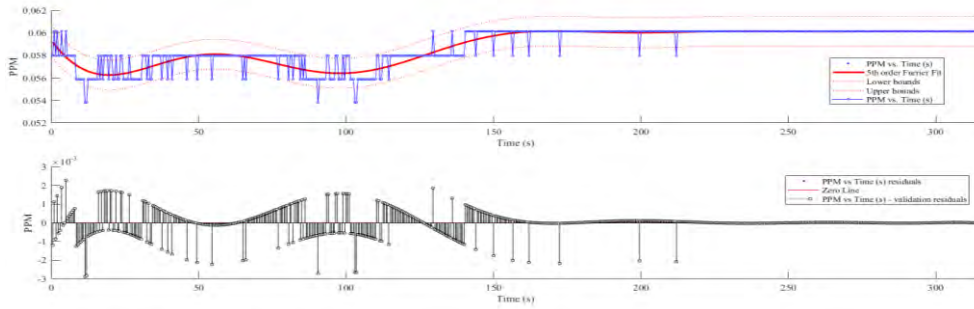
$$(11) \quad \mathcal{F}^{-1}[\mathcal{F}\{R(\tau)\}] = R(\tau).$$

Let $f(x)$ and $h(x)$ be two functions, and $h(x)$ convolutes with $f(x)$. Then the resultant function can be termed as $g(i)$. Mathematically,

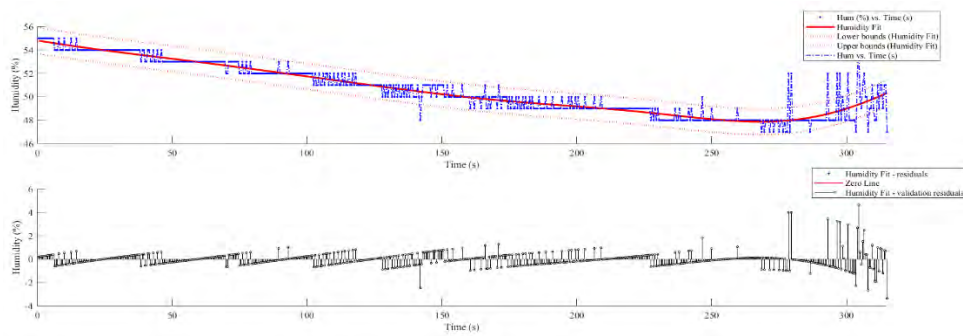
$$(12) \quad g(i) = f(x) \otimes h(x) = \int_{-\infty}^{\infty} f(x) \cdot h(i - x) dx.$$

The resultant function $g(i)$ has some unique identity rather than both $f(x)$ and $h(x)$. It can be also written as

$$(13) \quad g(i) = f(x) \otimes h(x) = \int_{-\infty}^{\infty} f(x) \cdot h(i - x) dx.$$



(a)



(b)

Fig. 8. Processed Signal (Humidity vs Time) (a); Humidity vs Time domain graph with 8th order Furrier transform using 95% of confidence limit (b)

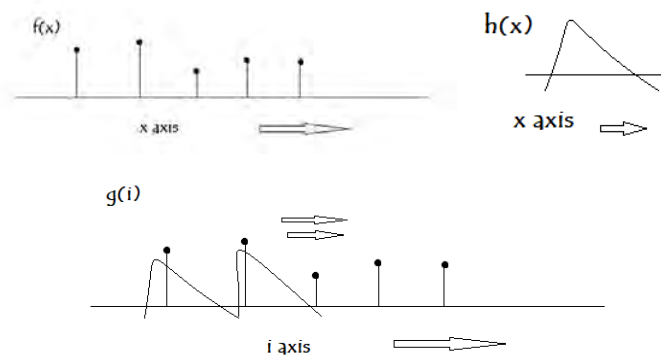


Fig. 9. Graphical representation of convolution theorem

Fig. 9 depicts the graphical representation of $f(x)$ convoluting $h(x)$ forming a new function $g(x)$ which follows the Equations (9)-(13). Fig. 10 shows the

experimental data-logged graphs from three identical gas sensors placed in different places inside the experimental control volume.

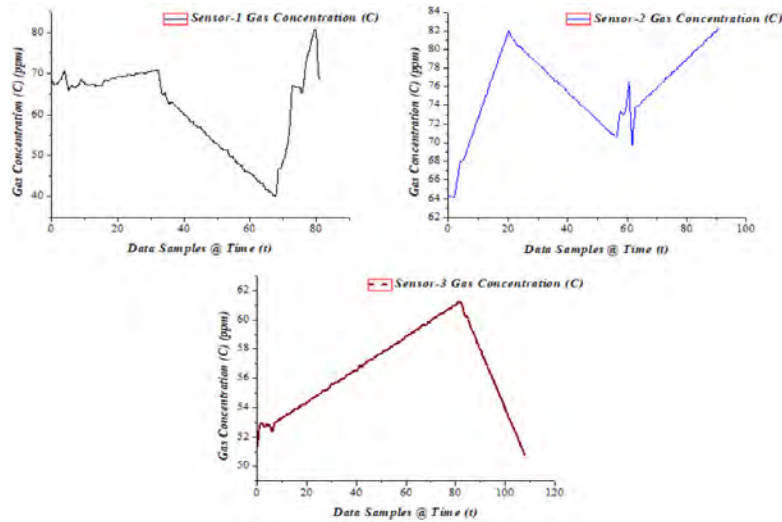


Fig. 10. Gas concentrations of three different nodes inside the control volume (raw data)

Now, those sensed data are correlated using the *fx-corr* command used for auto-correlation in MATLAB. The lags in Sensor-1, Sensor-2 and Sensor-3 are calculated with respect to two sensors' data at a time. Fig. 11 shows the graph of lagged data for the three sensors.

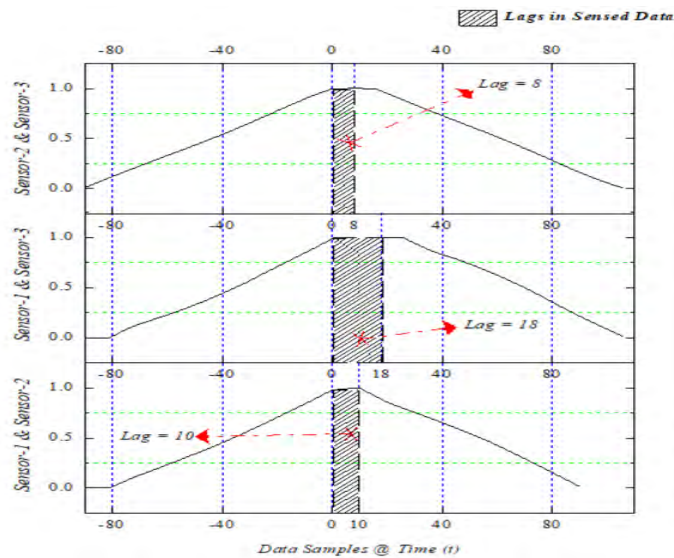


Fig. 11. Lags in logged data from multiple identical sensors (correlated samples)

Now, it is clear from Fig. 11 that using multiple sensors simultaneously can be followed by unnecessarily-logged data. Thus, correlation is very necessary for aligning sensors data in a mannered way. It is only possible when the sensors are

collecting samples at the same sampling frequency that in this research was 11.52 kHz or 115,200 baud/samples. From Equation (13), the correlated data can be plotted (Fig. 12) with respect to time or samples.

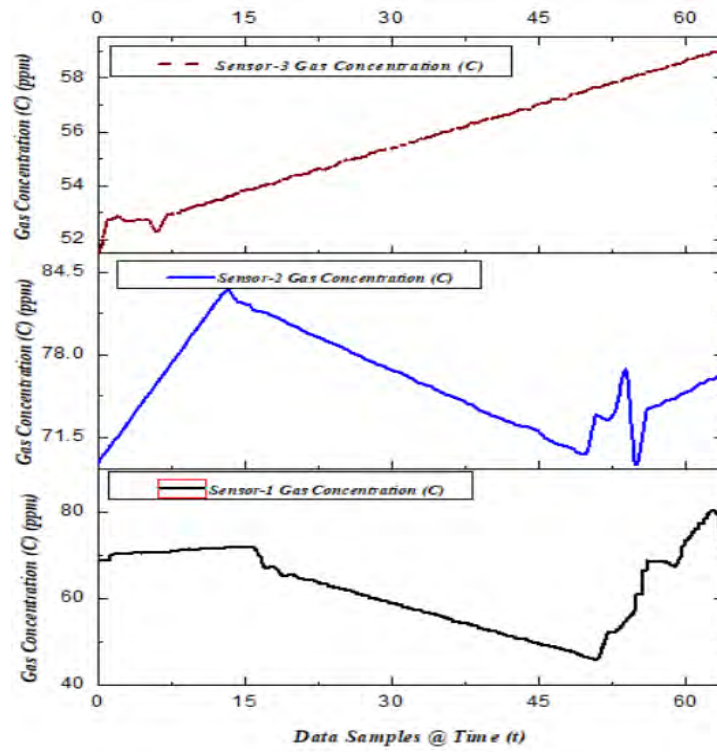


Fig. 12. Correlated signals from multiple of three gas sensors

Fig. 13 shows the actual & experimental Sensitivity vs Concentration plot, from where it can be said that the calibration was 90-95% accurate, which is good.

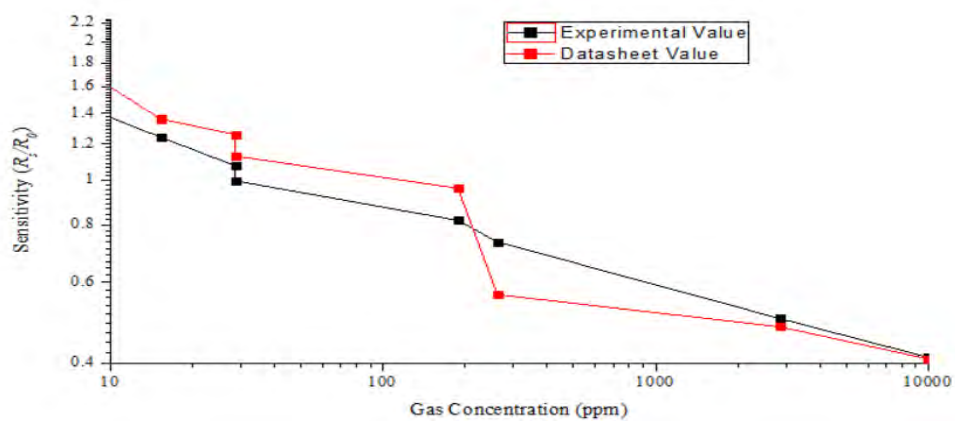


Fig. 13. Sensitivity vs PPM graph (Log-Log plot)

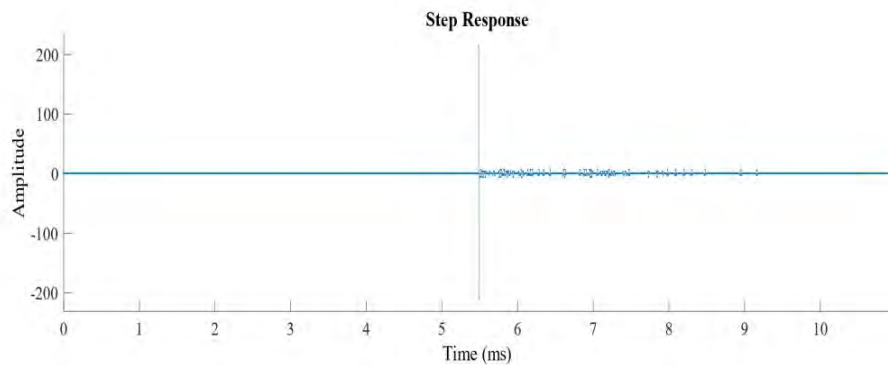


Fig. 14. Step response

From Fig. 14, the step response can be shown where it is seen that initially the system runs fine but after a certain period it shows some abrupts but the statistical filter automatically fixes the errors resulting in a smooth response. Fig. 15 shows the experimental relation between supplied voltage and gas concentration.

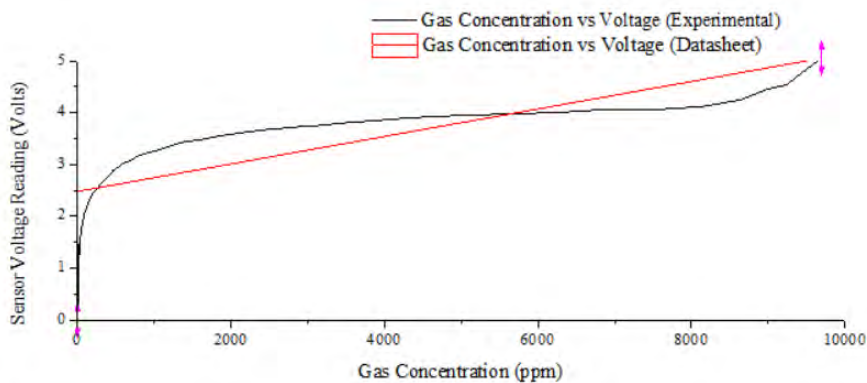


Fig. 15. Voltage vs PPM graph

5. Adaptive controls for experimental system

Feedback and Feedforward both control options were applied to the experimental prototype. Combining these two control options is the most challenging part of this research. The experimental threshold for gas sensor was set 300 ppm. For the feedback control, when the nearby gas concentration crosses 300 ppm then the controller automatically will set the actuator off for a certain delay period and rechecks the value of sensor again and again. If the value goes below 300 ppm then again for a certain period the actuators are turned on by a digital signal, but if again the gas concentration crosses 300 ppm then the system detects a gas leakage problem and the source valve is turned off.

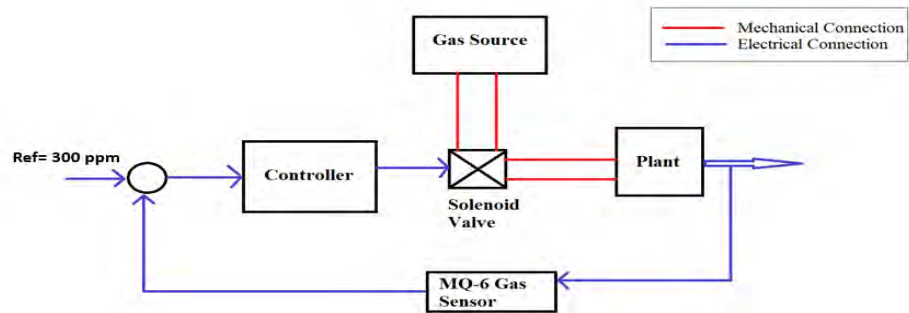


Fig. 16. Feedback control for proposed system

Fig. 16 shows the schematic of the developed feedback control system of the experimental system. In this device, the mean error will be the mathematical summation of Desired voltage and measured voltage and those two voltages are different in terms of signs. The desired value will be always positive, and the measured value is always negative. So, when those two values are equal but opposite in signs, so there will be no errors in the control system and that will be an absolute equilibrium condition [25, 26 and 27]. Thus, this type of feedback control system is very effective to use.

Feedforward control in simple terms mean controlling something by the aid of a manual signal. In this research, when feedback control crashes or manual switching is needed then from the server a predefined signal is sent to the controller and selected actuators can be controlled. Fig. 17 shows the schematic of the applied feedforward mechanism for controlling actuators using manual command over IoT.

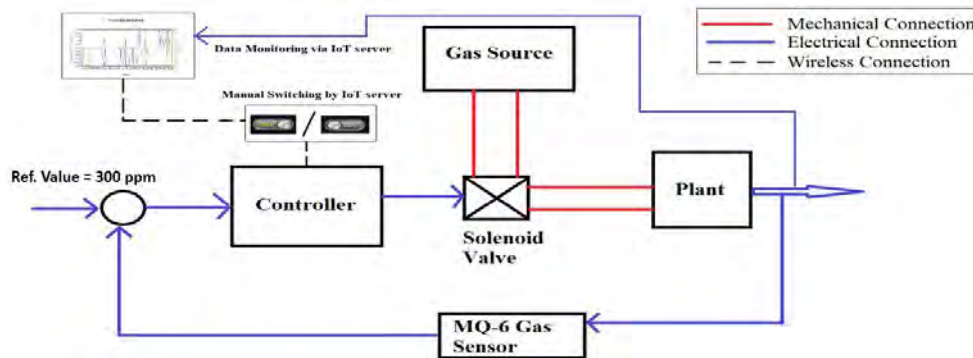


Fig. 17. Feed forward control system for the experimental setup

The feedforward controlling actions is implemented using “https-request” protocol used for single way communication. The control algorithm for this research has been formulated through some logical reasonings followed by C++ code maintaining the fuzzy logics given in Table 2.

From the Fuzzy logics, nine probabilities of actuation is possible by generating C++ code upon those logics, where two variables namely “https-request” (Feedforward command 1 or 0, if undefined, set value == 0) and “Gas concentration” (Reference value <300 == 0, >300 == 1, if value = 300, set value == 0) are liable to specified controller responses followed by a series of change in actuation

commands from controller utilizing both feedback and feedforward control actions simultaneously.

Table-2. Control Logics topology for proposed system

Logic	“https-request” from server (Str.)	Gas concentration (ppm)	Controller response (Bin)	Actuator output (Bin)
Logic-1	0	<300	0	0
Logic-2	0	>300	1	1
Logic-3	1	>300	1	1
Logic-4	1	<300	1	1
Logic-5	Undefined (== 0)	<300	0	0
Logic-6	Undefined (== 0)	>300	1	1
Logic-7	0	=300	0	0
Logic-8	1	=300	1	1
Logic-9	R	0	Reset	1

6. System performance & Guest user interface

To make a system performance analysis total 20 trials have been made. The trials were successfully investigated, and no major error was observed. The investigations were carried out according to [28] and [29]. The below Table 3 shows the performance test results. In this investigation, the commands were performed using the cloud-server followed by observation in actuation using the experimental setup described earlier in Fig. 3 by the mobile application which was referred from [30] based on fuzzy logic analysis. Fig. 18 represents the system performance test outputs in a graphical manner.

Table 3. System performance data table

No of Obs.	Gas concentration	HTTPS input	Actuator response	Elapsed time, s	Experimentation
1	170 (== 0)	0	0	0 (start)	Success
2	173 (== 0)	1	1	15.3	Success
3	211 (== 0)	0	0	20	Success
4	288 (== 0)	1	1	11	Success
5	316 (== 1)	0	1	7.5	Success
6	375 (== 1)	1	1	N/A	No Specified Change
7	402 (== 1)	0	1	N/A	No Specified Change
8	287 (== 0)	1	1	12	Success
9	255 (== 0)	1	1	N/A	No Specified Change
10	221 (== 0)	0	0	15.7	Success
11	300 (== 0)	0	0	N/A	No Specified Change
12	300 (== 0)	1	1	13.4	Success
13	302 (== 1)	2	1	Error processing	Error
14	380 (== 1)	4	1	Error processing	Error
15	293 (== 0)	0	0	12	Success
16	319 (== 1)	R	Reset	N/A	Reset of process
17	327 (== 1)	1	1	18	Success
18	289 (== 0)	0	0	8	Success
19	294 (== 0)	1	1	11	Success
20	277 (== 0)	0	0	5	Success

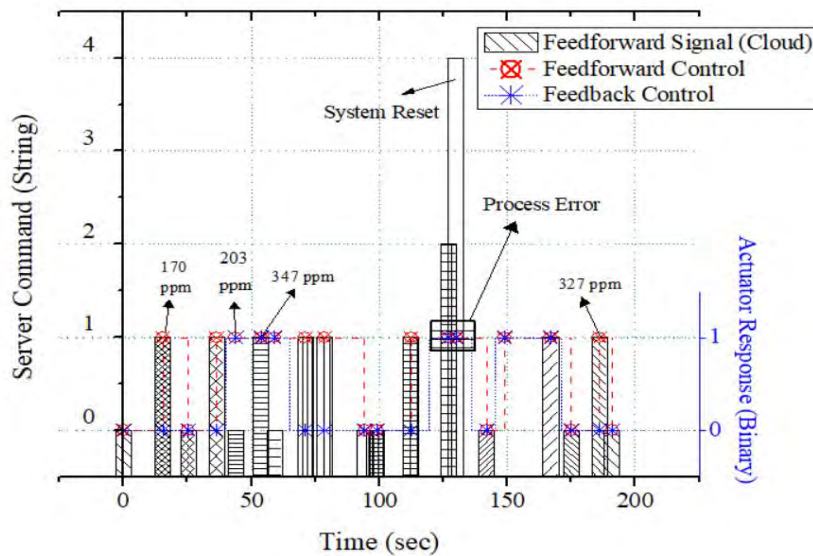


Fig. 18. Feedback and Feedforward control from system performance test

The evaluation shows that as a whole the system behaves like an error free system. Though the data processing time is a bit long (avg. 13 s), the system behavior seemed better. This system processing delay can be optimized by using manual api and custom server. As “Thingspeak” gives free access to students limiting browsing speed; so, no one can misuse it for commercial purpose. Fig. 19 below shows the graphical states of those experimental setup.

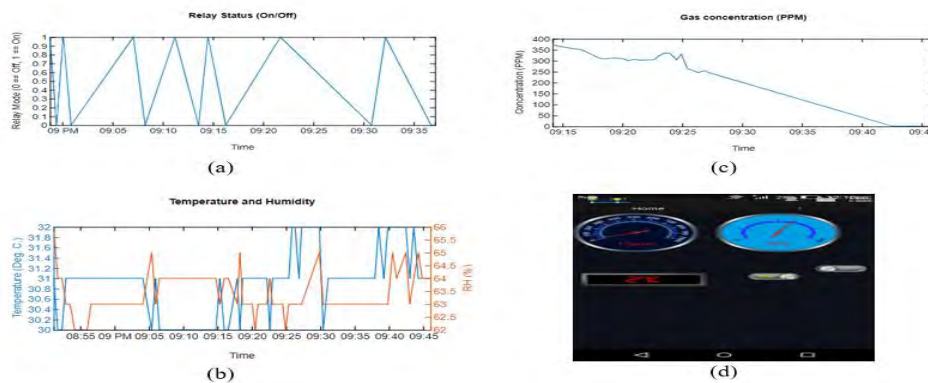


Fig. 19. Graphical presentation of monitored data: Relay state data (a); Temperature and RH data (b); ppm Concentration of LPG gas (c); Android application GUI (d)

This fabricated system can be used to prevent accidents caused by gas leakage in home and industry. Various types of toxic hydrocarbon-based gases (may have ability to ignite fire) are widely used in processes in food, chemical and fertilizer industries thus making the industries more viable to accidents due to unnoticed leakage of those gases. The fabricated prototype has almost 95% efficiency along with both feedback and feedforward control options which makes it more stable to

monitor and prevent unnoticed gas leakage crossing a defined reference value. The implemented cloud server controlling (feedforward) actions prove the system's infinite (very long range) distance actuating capability but it is very necessary to get connected with ISP for both controllers (Transmitter and Receiver).

7. Conclusion

The fabricated system runs successfully and 20 trials were performed to measure its performance. It showed no errors in those 20 trials, which took almost 3 hours to execute. The control system took almost 13 seconds to perform necessary commands until signals came from the host server. This delay period can be overcome by using the premium version of "Thingspeak" server. This delay period can be shortened up to 4 seconds as it is the minimal period of IoT server refreshing. It is apparent from analyzed signals that the impulse response and the group delay response seem quite perfect if the Baud Rate (Sampling Frequency) tuning ranges from 11 up to 12.6 kHz. In this study, 11.52 kHz Sampling Frequency is used. The power density spectrum of gas sensor is quite fine although the Signal to Noise ratio is comparatively higher. This can be overcome by using a 20 pF ceramic disk capacitor as it can work as a low pass filter. The overall system efficiency was about 95%, which is quite good for a robust controlling operation.

Acknowledgements: The authors are very grateful to the Department of Mechanical Engineering, RUET and the Department of Marine Engineering, Marine Fisheries Academy for the technical supports and laboratory facilities provided to complete this research. The authors are thankful to Dr. Mhia Md Zaglul Shahadat (Professor, Department of Mechanical Engineering, RUET) for his kind supports and supervision for the success of this research. They would also like to thank Marine Fisheries Academy as well as Ministry of Fisheries and Livestock, Government of the People's Republic of Bangladesh for granting funds to support this research.

References

1. Wang, J., M. Tong, X. Wang, Y. Ma, D. Liu, J. Wu, D. Gao, G. Du. Preparation of H₂ and LPG Gas Sensor. – Sensors and Actuators B: Chemical, Vol. **84**, 2002, pp. 95-97.
2. Amin, M. M., M. A. A. Nugratama, A. Maseleño, M. Huda, K. A. Jasmí. Design of Cigarette Disposal Blower and Automatic Freshner Using mq-5 Sensor Based on Atmega 8535 Microcontroller. – International Journal of Engineering & Technology, Vol. **7**, 2018, No 3, pp. 1108-1113.
3. Sinha, N., K. E. Pujitha, J. S. R. Alex. Xively Based Sensing and Monitoring System for IoT. – In: International Conference on Computer Communication and Informatics (ICCCI'15), IEEE, 2015, pp. 1-6.
4. Mallik, A., S. A. Hossain, A. B. Karim, S. M. Hasan. Development of LOCAL-IP Based Environmental Condition Monitoring Using Wireless Sensor Network. – International Journal of Sensors, Wireless Communications and Control, Vol. **9**, 2019, No 4, pp. 454-461.
5. Keshamoni, K., S. Hemanth. Smart Gas Level Monitoring, Booking & Gas Leakage Detector over IoT. – In: Proc. of IEEE, 7th International Advance Computing Conference (IACC'17), IEEE, 2017, pp. 330-332.

6. Mallik, A., A. Ahsan, M. M. Z. Shahadat, J. C. Tsou. Man-in-the-Middle-Attack: Understanding in Simple Words. – International Journal of Data and Network Science, Vol. 3, 2019, No 2, pp. 77-92.
7. Yadav, V., A. Shukla, S. Bandra, V. Kumar, U. Ansari, S. Khanna. A Review on Iot Based Hazardous Gas Leakage Detection & Controlling System Using Microcontroller & Gsm Module. – Journal of VLSI Design and Signal Processing, Vol. 3, 2017, No 1.
8. Sharma, M., D. Tripathi, N. P. Yadav, P. Rastogi. Gas Leakage Detection and Prevention Kit Provision with IoT. – Gas, Vol. 5, 2018, No 02.
9. Kukade, M. V., A. J. Moshayedi, D. C. Gharpure. Electronic-nose (E-nose) for Recognition of Cardamom, Nutmeg and Clove Oil Odor. – Electron. Its Interdiscip. Appl. (NCAEIA-2014), 2014.
10. Alekseev, V. V., V. S. Konovalova, E. N. Sedunova. Information-Measurement and Control System “Smart House” as Object of Practice-Oriented Training of Master’s Degree “Instrumentation Technology”. – In: 2017 International Conference, Quality Management, Transport and Information Security, Information Technologies (IT&QM&IS’17), IEEE, 2017, pp. 612-615.
11. Sabilla, S. I., R. Sarno, J. Siswanto. Estimating Gas Concentration Using Artificial Neural Network for Electronic Nose. – Procedia Computer Science, Vol. 124, 2017, pp. 181-188.
12. Tsang, Y. P., K. L. Choy, C. H. Wu, G. T. S. Ho, H. Y. Lam, P. S. Koo. An IoT-Based Cargo Monitoring System for Enhancing Operational Effectiveness under a Cold Chain Environment. – International Journal of Engineering Business Management, Vol. 9, 2017.
https: boi.org/10/177/1847979017749063
13. Karim, A. B., A. Z. Hasan, M. M. Akanda. Monitoring Food Storage Humidity and Temperature Data Using IoT. – MOJ Food Process Technol., Vol. 6, 2018, No 4, pp. 400-404.
14. Shahadat, M. M. Z., A. Mallik, M. M. Islam. Development of an Automated Gas-Leakage Monitoring System with Feedback and Feedforward Control by Utilizing Iot. – Facta Universitatis, Series: Electronics and Energetics, Vol. 32, 2019, No 4, pp. 615-631.
15. Brandt, A. A Signal Processing Framework for Operational Modal Analysis in Time and Frequency Domain. – Mecha. Sys. Sig. Process., Vol. 115, 2019, pp. 380-393.
16. Young, E. D., K. Strom, A. F. Tsue, J. L. Usset, S. MacPherson, J. T. McGuire, D. R. Welch. Automated Quantitative Image Analysis for Ex Vivo Metastasis Assays Reveals Differing Lung Composition Requirements for Metastasis Suppression by KISS1. – Clinical & Experimental Metastasis, 2018, pp. 1-10.
17. Mariani, S., L. Tarokh, I. Djonglic, B. E. Cade, M. G. Morricale et al. Evaluation of an Automated Pipeline for Large-Scale EEG Spectral Analysis: The National Sleep Research Resource. – Sleep Medicine, Vol. 47, 2018, pp. 126-136.
18. Zawawi, T. N. S. T., A. R. Abdullah, W. T. Jin, R. Sudirman, N. M. Saad. Electromyography Signal Analysis Using Time and Frequency Domain for Health Screening System Task. – Int. J. Hum. Technol. Inter., Vol. 2, 2018, No 1, pp. 35-44.
19. Gres, S., P. Andersen, C. Hoen, L. Damkilde. Orthogonal Projection-Based Harmonic Signal Removal for Operational Modal Analysis. – In: Structural Health Monitoring, Photogrammetry & DIC, Vol. 6, Springer, Cham, 2019, pp. 9-21.
20. Regalia, P. Adaptive IIR Filtering in Signal Processing and Control. Routledge, 2018.
21. Boashash, B., A. Aïssa-El-Bey, M. F. Al-Sa’d. Multisensor Time-Frequency Signal Processing MATLAB Package: An Analysis Tool for Multichannel Non-Stationary Data. SoftwareX, 2018.
22. Cohen, A. E. Automated HDL Signal Processing Deployment Performance from High Level MATLAB Specification for an Unmanned Aerial Vehicle (UAV). – In: Computing and Communication Workshop and Conference (CCWC’18), 2018 IEEE 8th Annual, IEEE, 2018, pp. 900-905.
23. Van Drongele, W. Signal Processing for Neuroscientists. Academic Press, 2018.
24. Anchal, A., A. Jain, S. Ahmad, P. K. Krishnamurthy. Nonlinearity Mitigation in Coherent Optical Communication Systems: All-Optical and Digital Signal Processing Approaches. – In: Selected Topics in Photonics, Springer, Singapore, 2018, pp. 41-51.

25. Yılmaz, U., A. Kircay, S. Borekci. PV System Fuzzy Logic MPPT Method and PI Control as a Charge Controller. – Renew. Sus. Ener. Rev., Vol. **81**, 2018, pp. 994-1001.
26. He, W., T. Meng, D. Huang, X. Li. Adaptive Boundary Iterative Learning Control for an Euler–Bernoulli Beam System with Input Constraint. – IEEE Trans. Neu. Net. Learn. Sys., Vol. **29**, 2018, No 5, pp. 1539-1549.
27. Walczak, S. Artificial Neural Networks. – In: Advanced Methodologies and Technologies in Artificial Intelligence, Computer Simulation, and Human-Computer Interaction, IGI Global, 2019, pp. 40-53.
28. Dworkniczak, P. Some Applications of Intuitionistic Fuzzy Sets for the Determination of a Sociometric Index of Acceptance. – Cybernetics and Information Technologies, Vol. **12**, 2012, No 1, pp. 70-77.
29. Pavlova, K., T. Stoilov, K. Stoilova. Bi-Level Model for Public Rail Transportation under Incomplete Data. – Cybernetics and Information Technologies, Vol. **17**, 2017, No 3, pp. 75-91.
30. Radeva, I. Multicriteria Fuzzy Sets Application in Economic Clustering Problems. – Cybernetics and Information Technologies, Vol. **17**, 2017, No 3, pp. 29-46.

Received: 10.08.2019; Second Version: 16.12.2019; Accepted: 27.12.2019